Journal of Russian Laser Research, Volume 19, Number 2, 1998

COMPLEX FERMI-PASTA-ULAM RECURRENCE AND THE PROBLEM OF INFORMATION STORAGE IN A NEURON

A. A. Berezin,[1] M. Garber,[1] and V. A. Shcheglov[2]

[1] *Oil and Gas Research Institute, Leninskii Pr. 65, Moscow 117924, Russia*
[2] *P. N. Lebedev Physical Institute, Russian Academy of Sciences, Leninskii Pr. 53, Moscow 117924, Russia*

Abstract

A qualitative model of a neuron was studied theoretically and experimentally. A coupled system of nonlinear Schrödinger (NLS) and sine-Gordon equations was used for mathematical description of the complex Fermi–Pasta–Ulam recurrence interpreted as a principal information carrier in the model. Computer and analog experiments were devised to verify the proposed concept.

1. Introduction

Traditionally, electrical activity of a single neuron is described within the framework of the Hodgkin–Huxley model [1]. In this case, in accordance with the Hartley formula, the memory capacity of a single spike amounts to $\log_2 2 = 1$. In other words, a neuron is treated as a system with two states, and all the complexity of the brain's ability to process information is explained by the presence of numerous parallel processing paths. However, correlations between learning and variations in concentrations of ribonucleic acid (RNA) and certain proteins in neurons were reported [2]. These data confirmed a hypothesis [3] that a single neuron, depending on the number of triplets in its RNA molecule, can have a memory capacity of up to 10 bit.

The purpose of this paper is to develop a neuron model based on the complex Fermi–Pasta–Ulam (FPU) recurrence spectrum, which is treated as an information carrier. The FPU recurrence phenomenon was first observed in 1955 [4] as a result of computer simulation of the oscillatory dynamics in a chain of nonlinearly coupled vibrators with fixed ends. In contrast to expectations, this system did not exhibit a tendency toward equipartition of energy among its degrees of freedom. Instead, a periodic recurrence of the initial perturbation energy spectrum was observed. Later [5], it was ascertained that the FPU phenomenon has two types of recurrence: simple and complex. In the case of the simple recurrence, an almost perfect periodic return of energy spectra is observed in the system, whereas, in a complex version, the periods are not stable and the Fourier modes exhibit complex sharing and regrouping of energy. This interesting behavior of the FPU chain stimulated a number of investigations of the system [6–9]. The first theoretical description of the problem was suggested by Zabusky and Kruskal [10] who showed that FPU recurrence can be defined by the Korteweg–de Vries (KdV) equation with periodic initial conditions. Another team of researchers, Yuen and Lake, were able to describe FPU recurrence within the framework of the nonlinear Schrödinger equation (NLS) with periodic boundary conditions [11]. The same authors reported a very interesting property of FPU recurrence, i.e., the ability to "memorize" the initial conditions for the active modes of its spectrum, reproducing them periodically in the FPU spectrum. In another study of the FPU problem [12], it was proposed that the exchange of energy between modes of the system is related to a transition to pronounced stochastisity. In discussing early investigations of FPU recurrence, it is necessary to emphasize that the original vibrator's chain had fixed ends [4]. However, even with open ends, the chain can also constitute a theoretically interesting autonomous distributed system, responsive to initial perturbations. Our attempt

Translated from a manuscript submitted December 1, 1997.

 1071-2836/98/1902-0194$20.00

to investigate the FPU dynamics in a chain with open ends brought us to the conclusion that a simple FPU recurrence [13] could be observed only in a chain of three equimass particles having both vertical and horizontal oscillatory degrees of freedom. An increase in the number of particles resulted in transition to complex FPU recurrence. The dynamics of the open-ended vibrator chain can be related to the behavior of a bouncing ball on a vibrating platform [14]. It can be demonstrated that this is not a chaotic system as some researchers suggested; rather, to a certain extent, it can be treated as a complex FPU recurrence phenomenon.

As the first step of our study, we attempted to consider neural activity using a plasma approach.

2. A Model for Electrical Activity of a Neuron

We will treat a neuron as a volume containing a strong electrolyte solution of intracellular fluid in which the RNA molecule acts as a neural information carrier. We also assume that all potassium ions in the solution are neutralized by forming ionic couples with hydroxyl groups K^+OH^-, which provides an overbalance of protons in the electrolyte solution. These assumptions allow us to analyze the proton-concentration dynamics in terms of the simplified cluster model of the seawater electrolyte as suggested by Frank and Wen [15]. According to this model, every sodium ion is surrounded by an ionic atmosphere consisting of four H_2O molecules and every chlorine ion has two H_2O molecules in its atmosphere (Fig. 1). In a spherical volume of a neuron, let us identify a one-dimensional chain of Na^+ and Cl^- ions near the inner layer of neuron membrane as illustrated in Fig. 1. Depolarization of the membrane gives rise to a proton-concentration wave due to the nonlinear mechanism of proton transport between H_2O molecules, as suggested by Bernal [16]. The electric potential φ_H generated by the combined sodium ion and the chlorine ion atmosphere can be defined within the framework of the Debye–Hückel theory as a sum of repelling and attracting components [16]:

$$\varphi_H = \frac{a}{b}\left(e^{-br_n} - 1\right) + ar_n. \tag{1}$$

Here, $b = \sqrt{\dfrac{8\pi n_0}{\varepsilon kT}}$, $a = \dfrac{e^2}{\varepsilon r_0}\sqrt{\dfrac{8\pi n_0}{\varepsilon kT}}$, e is the elementary charge, n is the sodium ion concentration, ε is the permittivity of water, r_0 is the distance between sodium and chlorine ions in the chain, and $r_n = x_n - x_{n-1}$, where x_n is the nth proton shift in the chain.

In view of (1), we can write an equation describing the dynamics of the proton motion in the chain (Fig. 1) in the form of Toda's chain [17] as

$$m_H \frac{d^2x_n}{dt^2} = a\left[e^{-b(x_{n+1}-x_n)} - e^{-b(x_n-x_{n-1})}\right], \tag{2}$$

where m_H is the proton rest mass.

Toda demonstrated [17] that Eq. (2) can be reduced to the KdV equation; as a result, we have

$$\frac{\partial u_H}{\partial \tau} - 6u_H\frac{\partial u_H}{\partial \xi} + \frac{\partial^3 u_H}{\partial \xi^3} = 0, \tag{3}$$

where $u_H = 2br_n$, $\xi = \dfrac{x - c_H t}{h_t}$, $h_t = \dfrac{x}{n}$, $c_H = h_t\sqrt{\dfrac{ab}{m_H}}$, and $\tau = \dfrac{c_H t}{24h_t}$.

The spherical shape of a neuron results in periodic boundary conditions for the proton concentration wave, as given by

$$u_H(\xi, \tau) = u_H(\xi + L_n; \tau), \tag{4}$$

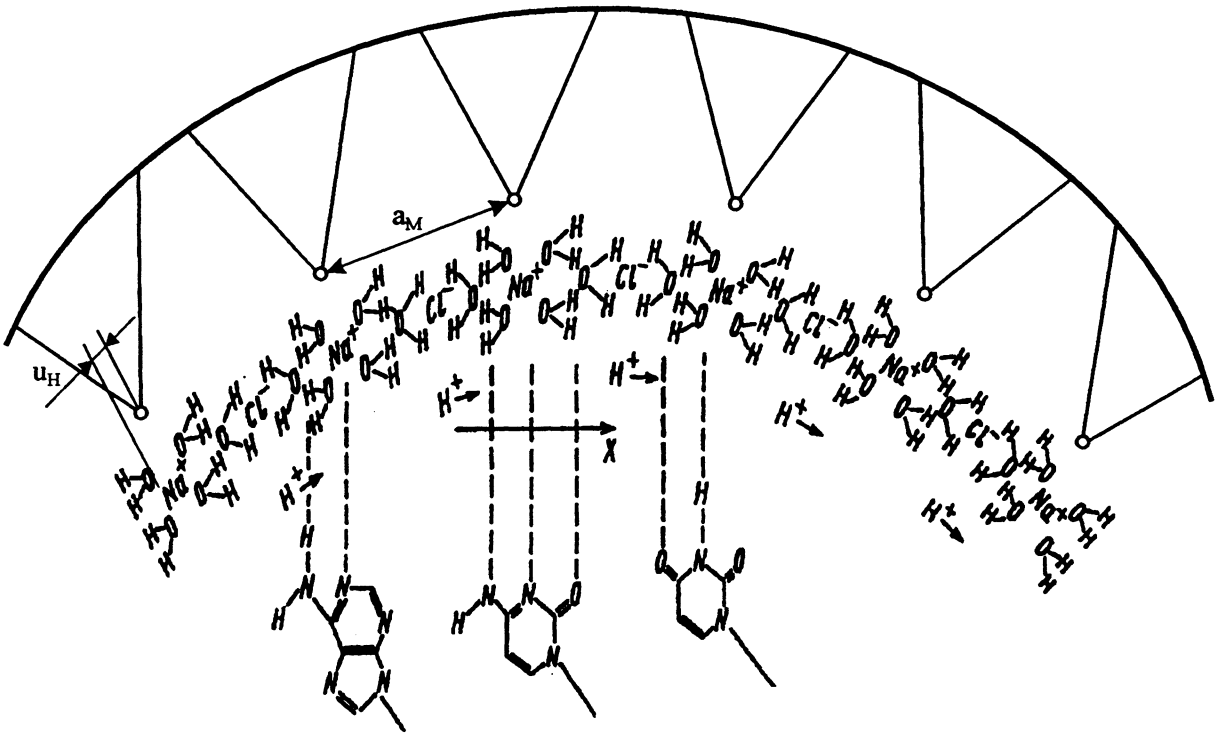

Fig. 1. Formation of a proton concentration wave in a neuron. The RNA triplet.

where $L_n = 2\pi R_n$ with R_n being the inner radius of a neuron. Zabusky and Kruskal demonstrated [10] that Eq. (3) combined with Eq. (4) yields a solution in the form of the FPU recurrence. In the proposed model, the periodic boundary conditions for the proton wave can be modulated in accordance with the nucleotide sequence of the RNA molecule (Fig. 1).

We can now evaluate numerically the neuron memory capacity with allowance for strong-electrolyte properties of the intracellular fluid. Assuming that the distance of proton hop between the neighboring H_2O molecules is equal to 0.86 Å and the temperature of the intracellular fluid is $T = 310$ K, we can use the analogy with a plasma to define the rate of collisions of protons with H_2O molecules as

$$v_c = \frac{V_H}{\lambda_H} = \frac{1}{\lambda_H}\sqrt{\frac{kT}{m_H}}, \tag{5}$$

where λ_H is the proton free path length and V_H is the proton velocity.

Since the duration of a nerve impulse amounts to several milliseconds [18], we can formally evaluate the single spike memory capacity with the use of Kotel'nikov's theorem [19] as follows:

$$N_{sc} = 2v_c\tau_i = 3.72 \cdot 10^{10} \text{ bit/spike}. \tag{6}$$

The next step is to show how this high-frequency signal can be embedded into the structure of the action potential. With this in mind, we consider a neuron membrane as a liquid crystal containing a lipid bilayer [20]

(Fig. 1). Taking into account that the distance between the lipid molecules in the membrane layer and the distance between sodium ions in the chain (Fig. 1) are about 4.7 Å [16, 21], we may suggest the following mechanism of interaction between high-frequency proton-concentration wave and the low-frequency ionic wave of the action potential.

We consider the sodium chain shifted by a distance U_n relative to the equilibrium positions of the lipid molecules of the membrane inner layer (Fig. 1). In this case, we can use the approach developed by Frenkel and Kontorova [22] for the analysis of the dynamics of dislocations in crystals.

We define the potential affecting the nth sodium ion from the immovable chain of lipid molecules in the neuron membrane layer (Fig. 1) as

$$U(U_n) = U_0\left(1 - \cos\frac{2\pi U_n}{a_L}\right), \tag{7}$$

where a_L is the distance between neighboring lipid molecules in the membrane layer and U_0 is the relative position of the lipid molecule.

In this case, the dynamics of the sodium-ion shift can be defined by the following equation [23]:

$$m_{\mathrm{Na}}\frac{d^2U_n}{dt^2} + \rho(2U_n - U_{n-1} - U_{n+1}) + \frac{\pi U_0}{a_L}\sin\left(\frac{2\pi U_n}{a_L}\right) = 0. \tag{8}$$

Here, ρ is the elastic constant for the relative shift of the sodium ions.

Using the continuum approximation in the limit of $U_n(x,t) \to U(x,t)$ and introducing the function (proportional to the modulation of sodium ion density)

$$\varphi(x,t) = \frac{2\pi U(x,t)}{a_L}, \tag{9}$$

we arrive at the sine-Gordon equation

$$\frac{\partial^2\varphi}{\partial x^2} - \frac{1}{c_s^2}\frac{\partial^2\varphi}{\partial t^2} = \frac{1}{\lambda_0^2}\sin\varphi. \tag{10}$$

Here, $c_s = a_L\sqrt{\dfrac{\rho}{m_{\mathrm{Na}}}}$ is the velocity of longitudinal sound wave in the sodium-ion chain and $\lambda_0 = \dfrac{\rho^2}{2\pi}\sqrt{\dfrac{\rho}{U_0}}$ is the relative length of the chain.

Taking into account that the length of the sodium-ion chain is limited by the size of the neuron, we can derive a soliton solution to Eq. (10) as [24]

$$\varphi_s(x,t) = 4\arctan\left(\frac{c_s k}{\sqrt{2}a}\sec hkx\,\sin\omega t\right), \tag{11}$$

where $\omega^2 + c_s^2k^2 = c_s^2/\lambda_0^2$ is the dispersion relation.

The dimension of a neuron L_N defines the boundary conditions for Eq. (10) by analogy with a long transmission line open on both ends, which was used for simulation of the Josephson junction dynamics [25]; thus we have

$$\left.\frac{\partial\varphi}{\partial x}\right|_{x=0} = \left.\frac{\partial\varphi}{\partial x}\right|_{x=L_N} = 0. \tag{12}$$

As shown by Fulton [25] for chains with limited length described by the sine-Gordon equation, there exists an energy exchange between the soliton solution and the plasma solution. Thus, in the limiting case of $\sin\varphi \to \varphi$, a solution to Eq. (10) defines the standing waves which are similar to the conoidal waves following

from the KdV equation [26]. These properties of Eq. (10) make it possible to resort to the experimentally observed plasma phenomenon consisting in locking of the high-frequency electric field by the low-density plasma regions [27]. Within the framework of this approach, we may suggest that a spike locks the high-frequency proton-concentration waves within the body of the low-frequency sodium-ion-concentration waves because the strong electrolyte solution of the neuron intracellular fluid can be treated as a dense plasma. Thus, the formation of a nervous spike can be described by the following system of coupled sine-Gordon and KdV equations:

$$\begin{aligned} \frac{\partial^2 \varphi}{\partial x^2} - \frac{1}{c_s^2}\frac{\partial^2 \varphi}{\partial t^2} &= \frac{1}{\lambda_0^2}(1+\beta_1 u_H)\sin\varphi, \\ \frac{\partial u_H}{\partial \tau} - 6(1+\beta_2\varphi)u_H\frac{\partial u_H}{\partial \xi} + \frac{\partial^3 u_H}{\partial \xi^3} &= 0. \end{aligned} \tag{13}$$

Here, $\beta_1 < 1$ and $\beta_2 < 1$ are the parameters of interaction between sodium ion concentration waves and proton waves.

In accordance with the results obtained by Ikezi [27], who studied a similar couple of equations, a solution to system (13) defines a soliton with internal oscillatory structure. Taking also into account the results reported by Zabusky and Kruskal [10], we may conclude that the solution to Eq. (13) includes the FPU recurrence spectrum confined in the soliton defined by the sine-Gordon equation:

$$\varphi_B = 4\arctan\left[\frac{c_s k}{\sqrt{2\omega}}\sec h(kx + \Theta_i)\right]. \tag{14}$$

In Eq. (14), the two functions accounting for the dynamics of the FPU recurrence in a neuron have the following form:

$$\begin{aligned} \Theta_x &= \Theta_{0x}\sin(k_{\text{FPU}}x + \alpha_x), \\ \Theta_t &= \Theta_{0x}\sin(\omega_{\text{FPU}}t + \alpha_x). \end{aligned} \tag{15}$$

Here, k_{FPU} and ω_{FPU} are the spatial and temporal frequencies of the FPU recurrence. The structure of the FPU spectrum is defined by the properties of the nonlinear oscillatory processes occurring in the RNA molecule. The early stages reflect the arrangement of nucleotides in the RNA molecule.

3. Possible Role of RNA in the Storage of Neural Information

We now clarify in what form neural information can be represented within the framework of the proposed model.

In a series of papers [28–30], Hyden reported a correlation between learning on the one hand and RNA and protein changes in nerve cells on the other hand; he inferred that "brain protein and RNA synthesis are required for the establishment of long-term memory and that they occur during or shortly after learning." According to his hypothesis, the long-term memory capacity of a single neuron may be far in excess of that generally adopted in current neural network models and neural-science theories. In this section, we suggest a possible realization of postulates put forth by Hyden regarding the participation of RNA in neural information processing.

Formal numerical evaluation of memory capacity of the RNA molecule is based on the following assumptions: The memory capacity of the genetic code can be evaluated as $\log_2 20 \simeq 4.3$ bit per triplet. If we accept

Hyden's estimate of the cytoplasmic RNA content in a neuron [2], which is about $4 \cdot 10^{13}$ dalton, information stored in a single neuron can amount to over 10^{11} bit.

On the other hand, the RNA molecule may be interpreted as a network of interacting quantum oscillators. Each link of this chain includes one furanose ring coupled with one nitrogen base. Let us consider a simplified model of such a link, in which a nitrogen base is replaced by a benzene ring. According to [31], the quasi-local vibrational-mode frequency in the furanose ring is adiabatically dependent on the ring conformation, which has two stable states. Assuming both states to be equiprobable, we can define potential energy for a delocalized electron in the furanose ring as a double symmetric potential well with two minima:

$$U_e(U_{ne}) = \varepsilon_0 \left(1 - \frac{U_e^2}{U_{0e}^2}\right). \tag{16}$$

Here, ε_0 is the potential barrier height, U_e is the electron displacement from the peak of the barrier, and $\pm U_{0e}$ are the locations of the potential well minima.

Taking into account (16) and the expression for the one-dimensional chain sine-Gordon equation [32], we can deduce the equation defining the acoustic-wave dynamics in the furanose ring as

$$\frac{\partial^2 \varphi_e}{\partial t^2} - c_0^2 \frac{\partial^2 \varphi_e}{\partial x^2} + \omega_0^2 \sin \varphi_e = 0, \tag{17}$$

where φ_e is the magnitude of electron displacement in the furanose ring, c_0 is the velocity of sound, and ω_0 is the frequency defined by ε_0.

Since the furanose ring constitutes a discrete closed chain, the sine-Gordon equation (17) can be discretized and its solution will demonstrate energy distribution among many modes exhibiting the FPU recurrence [33]. In this particular case, we are dealing with quantum FPU dynamics for the energy of phonons of the acoustic waves in the ring.

The quantum dynamics of the benzene ring is formally related to a system with two states [34]. However, the actual pattern of the electric field in this molecule is more complex. One of the possible approaches to its analysis can be based on the wave packet dynamics. Wave functions with the least uncertainty $\Delta p \Delta q$ correspond to Gaussian distributions both in coordinate and momentum representations. Such functions are convenient as a basis for constructing many-particle complicated wave functions for atoms and molecules because overlap integrals and interaction matrix elements can be derived algebraically. In 1975, Heller [35] suggested a new application of the Gaussian curve to constructing the wave functions. He assumed that a classical trajectory in the phase space where the Hamiltonian in the immediate neighborhood of a moving point $p_t q_t$ at a given instant of time t can be expanded in powers of $(p - p_t)$ and $(q - q_t)$ to the second order as in the case of a harmonic oscillator. Then the wave function is given by

$$\psi(q,t) = \exp\left\{\frac{i}{\hbar}[\alpha(q - q_t)^2 + p_t(q - q_t) + \gamma]\right\}, \tag{18}$$

where α is a complex symmetric matrix with the number of rows and columns equal to the number of degrees of freedom and γ is a complex phase. The expectation values for the position and momentum are simply

$$\langle p \rangle = p_t \qquad \text{and} \qquad \langle q \rangle = q_t.$$

The matrix α defines the spread of the wave packet, which is related to the approximate shape of the Hamiltonian near $(p_t q_t)$. The complex phase γ provides the necessary normalization as well as the critical phase angle. The time dependences of α, p_t, q_t, and γ are deduced by inserting (18) into the Schrödinger equation. The potential energy is expanded to second order in $q - q_t$; thus, we have

$$V(q,t) = V(q_t,t) + V_q(q - q_t) + \frac{1}{2} V_{qq}(q - q_t)^2, \tag{19}$$

where the first and the second derivatives V_q and V_{qq} are to be taken at the point q_t and at the time instant t. The original idea of spreading a Gaussian wave packet (18) along a classical trajectory was implemented by Davis and Heller [36] in the Henon–Heiles model [37], but this time in the integrable domain. The main conclusion following from this approach is the distinction between the spectra of the Gaussian wave packets located in the integrable and the ergodic domains [38]. Apparently, we deal with such a situation in the benzene molecule. It is evident that the linear Schrödinger equation cannot describe this nonlinear dynamics. Taking into account the results obtained with the above-mentioned model and the fact that the kinetic energy is much lower as compared to the rest energy of electrons in the benzene ring, we can derive the nonlinear Schrödinger equation for interacting electron wave packets in the benzene molecule [39]:

$$i\frac{\partial\psi}{\partial t} + \frac{\partial^2\psi}{\partial x^2} - V(q)\psi = 0. \tag{20}$$

Here, $V(q) = \psi\psi^*$ is a nonlinear potential.

The nitrogen base also constitutes a discrete structure and this allows us to use the FPU approximation by means of the NLS equation [40]. Thus, the quantum FPU recurrence can exist in the nitrogen base as well.

Now, for the simulated elementary RNA molecule cell consisting of the coupled furanose ring and nitrogen base, the dynamics of interaction of the acoustic waves in the furanose ring with the electric waves in the benzene ring can be described by coupled sine-Gordon and nonlinear Schrödinger equations:

$$\begin{aligned} \frac{\partial^2\varphi_e}{\partial t^2} - c_0^2\frac{\partial^2\varphi_e}{\partial x^2} + \omega_0^2(1+\alpha_e|\psi|^2)\sin\varphi_e &= 0, \\ i\frac{\partial\psi}{\partial t} + d\frac{\partial^2\psi}{\partial x^2} - V(q)(1+\beta_e\varphi_e)\psi &= 0, \\ \alpha_e < 1, \quad \beta_e < 1, \qquad d = &\text{ const.} \end{aligned} \tag{21}$$

The system (21) appears as a nonlinear generalization of the Zakharov couple [41] aimed at describing the electroacoustic waves in a plasma. In the general case, the solution to the coupled system (21) represents a stable energy cluster of a soliton type with a internal oscillatory structure that can be interpreted as quantum FPU recurrence. Linking the elementary model cells (21) into the complete chain of the simulated RNA molecule, we can form a macro FPU chain for the energy distribution along the spatial coordinate:

$$\begin{aligned} \frac{\partial^2 W_n}{\partial x^2} &= (W_{n+1} - W_n) - (W_n - W_{n-1}) + a[(W_{n+1} - W_n)^3 - (W_n - W_{n-1})^3], \\ a &= \text{const.} \end{aligned} \tag{22}$$

Here, W_n is the energy of the $n(c)$th elementary cell defined by the sum of the squared amplitudes of a finite number of FPU spectrum harmonics.

The resulting quasi-periodic energy exchange between different modes of the RNA FPU recurrence spectrum is primarily defined by the structure of the molecules. In other words, changes in the benzene ring induced by the actual nitrogen base give rise to individual power density distributions of a particular molecule. Any new changes in the RNA molecule introduce new boundary conditions for the RNA FPU recurrence and thus provide the possibility of additional data recording into the vibrational dynamics of the molecule. It is evident that there is no limit for the body of information being recorded. All new information only complicates the existing FPU spectrum. The nonlinear character of the RNA model results in the interaction between micro (or quantum) and macro FPU recurrences in the RNA molecule. Later we will estimate the frequencies in both recurrences.

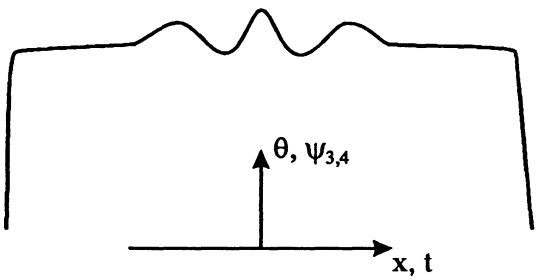

Fig. 2. Computer solution to the coupled NLS and sine-Gordon equations. Vertical axis: amplitude (in arbitrary units). Horizontal axis: spatial size of a soliton (in arbitrary units).

The information recorded in the RNA should next be transferred into the structure of a nervous spike. As was shown in the previous section, a circular ionic wave of action potential formed inside a neuron also represents FPU recurrence. The information contained in the FPU spectrum of a neural RNA molecule (Fig. 1) can be transferred through the electrolyte of neuron intracellular fluid to the internal spectrum structure of the spike. In other words, any activation of a neuron will result in transmission of the portion of information stored at the moment in vibrational form in the RNA molecule to the spike structure.

Facing evident difficulties in formalization of this mechanism, we resort to computer and analog simulation of the problem.

4. Computer Simulation

We performed a numerical simulation of a solution to system (21). The existing results of the Zakharov's couple study [41] allowed us to assume that the solution to (21) represents a low-frequency acoustic soliton, in which a high-frequency electric field is trapped. This form of solution has been experimentally verified by some researchers [27] for solitons in a plasma. We expected that the solution to (21) can involve the complex FPU recurrence.

System (21) was studied numerically with code written in Pascal. The choice of coefficients of couple (21) was governed by the desire to get a stable solution. As a result, the following values of the parameters were selected:

$$c_0 = 0.31, \quad \omega_0 = 0.1, \quad \alpha_e = 0.01, \quad d = 1.6, \quad V(g) = 18.2, \quad \beta_e = 5 \cdot 10^{-7}.$$

The resulting solution is shown in Fig. 2, where the amplitudes $\varphi_e > \psi$ are plotted on the vertical axis and the spatial coordinate is plotted on the horizontal axis.

As is evident from Fig. 2, the solution consists of the double soliton or breather solution of the sine-Gordon equation, which incorporates the high-frequency wave of NLS. The numerical analysis is also indicative of the existence of quasi-periodic recurrence in the internal structure of the breather.

The obvious incompleteness of the obtained numerical solution and the necessity to evaluate the effect of discretizing the equations of system (21) prompted us to resort to the corresponding analog simulation.

5. Analog Simulation

This experiment was aimed at the analog simulation of the RNA molecule model and also at the study of the interaction between RNA molecular vibrations and the action potential of a single neuron. For this purpose, we developed an electronic model of the RNA chain in the form of two coupled nonlinear distributed oscillatory systems consisting of two pairs of coupled transmission lines regenerated by two transistors. Every furanose ring was simulated by two turns of wires wound on a plastic toroidal core. Every benzene ring was also simulated by two turns in the other transformer wound on the same core. Four transmission lines of both transformers involved 36 turns each of 1-mm insulated wire quadded wound on the same toroidal plastic ring 60 mm in diameter and of thickness 12 mm with a common axis of 55 mm in length to form a strongly coupled pair of distributed resonators, which simulated the whole chain of the RNA molecule. Both lines of the first transformer were accessed from opposite ends and were connected to emitter and collector circuits of a transistor, which operated in the avalanche mode as a switch.

A second pair of lines was connected to the emitter and collector circuits in a corresponding way. In this case, both transistor junctions served as active distributed elements having a transfer function of the form

$$F_t(\omega_j) = A\frac{\sin(\pi\omega_j/\omega_{j0})}{\pi\omega_j/\omega_{j0}}, \tag{23}$$

where $\omega_{j0} = 2\pi\mu_p E_0/l_j$ is the resonance frequency, μ_p is the mobility of injected carriers, E_0 is the intensity of electric field applied to the junction, and l_j is the length of the junction.

In the suggested electronic model, every first pair of turns simulated the dynamics of acoustic vibrations in the furanose ring. Let us consider the function of electronic conductivity in both turns. Since the currents in these turns are almost equal but opposite, we can assume that all electrons providing conductivity in the crystal lattice of the conductor of each turn are free electrons. The motion of electrons in both turns can be described by two additively coupled linear Schrödinger equations [34]:

$$\begin{aligned} -\frac{\hbar^2}{2m_e}\frac{\partial^2\psi_1}{\partial r^2} + V(r)\psi_1(r) &= E\psi_1(r) - K\psi_2(r), \\ -\frac{\hbar^2}{2m_e}\frac{\partial^2\psi_2}{\partial r^2} + V(r)\psi_2(r) &= E\psi_2(r) - K\psi_1(r), \\ r &= x \pm z. \end{aligned} \tag{24}$$

Here, ψ_1 and ψ_2 are the wave functions of electrons in the crystal lattice of the first and the second turn, $V(r)$ is the potential energy in the electric field of the lattice, E is the total energy of electrons, $K\psi_1(r)$ and $K\psi_2(r)$ account for mutual interactions of both wave functions because of the Hall effect, and z is the lattice constant.

Due to opposite flow of electrons in both turns, the solutions to (24) have the following form [42]:

$$\begin{aligned} \psi_1 &= U_{k1}(r)e^{ir(k_1-k_2)}, \\ \psi_2 &= U_{k2}(r)e^{ir(k_1-k_2)}. \end{aligned} \tag{25}$$

Here, $U_{k1}(r)$ and $U_{k2}(r)$ are the Bloch functions, and k_1 and k_2 are the average wave numbers of electron waves in both turns.

Spatial beats occurring between electronic waves in both turns result in the following dynamics of electron density in every turn:

$$D_{1,2} = \frac{2k}{\hbar}|U_{k1}(r)U_{k2}(r)|\sin[r(k_1 - k_2)]. \tag{26}$$

The resulting magnetic field generated by the beating waves is given by

$$\begin{aligned} \frac{\partial \Theta}{\partial x} &= H, \\ \Theta &= r(k_1 - k_2). \end{aligned} \tag{27}$$

Such an approach allows us to draw the analogy with the Josephson junction [43] for the description of the electron density wave dynamics in every turn and to use the sine-Gordon equation as

$$c_e^2 \frac{\partial^2 \Theta}{\partial x^2} - \frac{\partial^2 \Theta}{\partial t^2} = \omega_e^2 \sin \Theta, \tag{28}$$

where c_e is the electron-related sound velocity in the crystal lattice of the conductors and $\omega_e = E/\hbar$ is the electron frequency.

Thus, the quantum-mechanical processes in the furanose ring are simulated by the dynamics of electron waves in every pair of turns of two distributed coupled oscillators.

Another pair of turns belonging to the second transmission line transformer simulated the dynamics of the electric field in the benzene ring. As distinct from the previous case, this time both lines were switched accordingly into the collector and emitter circuits of the transistor, forming a classical two-line coupled system with split frequencies and doubling of the number of resonance positions [44]. Based on the fact that the energies of these vibrations are equal and both waves are standing, we can consider the dynamics of wave processes in every turn in the following way: The resonance characteristics of p–n junctions (23) in both transistors give rise to electron wave packets in every turn. Splitting of energy levels induces modulation of the wave numbers near their average values.

It is necessary to emphasize that the system under consideration is similar, to a certain extent, to a couple of classical interacting quantum oscillators, in which the joint probability density periodically changes in time. However, in the model, the interaction of two wave packets results in mutual modulation of their wave numbers, which allows us to use the nonlinear Schrödinger equation for describing the electron wave function dynamics ψ_3 and ψ_4 of each turn of wires:

$$i\frac{\partial \psi_{3,4}}{\partial t} + d_p \frac{\partial^2 \psi_{3,4}}{\partial x^2} + k_m |\psi_{3,4}|^2 \psi_{3,4} = 0, \qquad d = \text{const}. \tag{29}$$

The interaction between the first and the second pairs of turns simulating the interaction between acoustic waves in the furanose ring and electric waves in the benzene ring can be written as

$$\begin{aligned} c_e^2 \frac{\partial^2 \Theta}{\partial x^2} - \frac{\partial^2 \Theta}{\partial t^2} &= \omega_e^2 \left(1 + \alpha_e |\psi_{3,4}|^2\right) \sin \Theta, \\ i\frac{\partial \psi_{3,4}}{\partial t} + d_p \frac{\partial^2 \psi_{3,4}}{\partial x^2} + k_m (1 + \beta_e \Theta) |\psi_{3,4}|^2 \psi_{3,4} &= 0, \\ \alpha_e < 1, \quad \beta_e < 1. & \end{aligned} \tag{30}$$

In order to derive the general resonance solution for both equations of the system (30), we can make use of the equality of energy in both pairs of turns and the dispersion relations for acoustic and electric waves; thus, we have

$$\frac{2\hbar\sqrt{\pi}c}{l_t} \left| \frac{\sin(k_m l_t/2)}{k_m} \right| = 2\hbar \sqrt{\frac{X_e}{m_e^*}} \left| \sin\left(\frac{\omega_0 a_e}{c_0}\right) \right|, \tag{31}$$

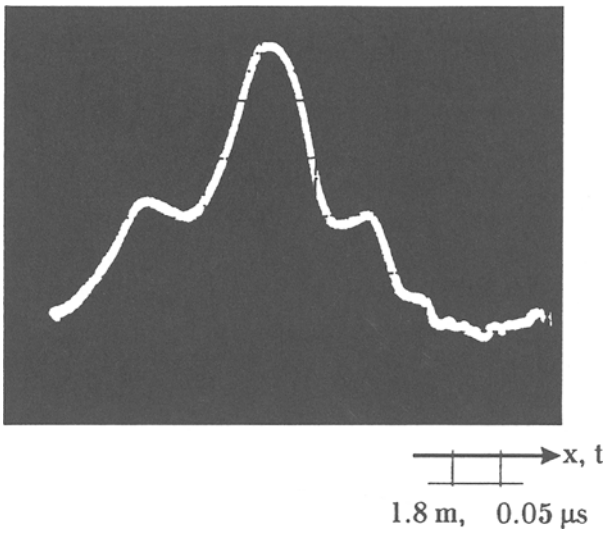

Fig. 3. The oscillogram of the voltage wave train illustrating the interaction between two pairs of lines wound on a plastic toroidal core. Vertical axis: 5 V per division. Horizontal axis: 0.05 μs per division.

where l_t is the length of the turn, X_e is the degree of collectivization of neighboring electrons, m_e^* is the effective electron mass, and a_e is the neighboring-atom distance in the crystal lattice of the conductor material.

Typical values of spatial k_m and temporal ω_e frequencies in the electronic model on the scale defined by the crystal-lattice parameters are $k_m = 16$ rad/m and $\omega_e/2\pi = 10^{16}$ Hz and, on the macroscale defined by the length of the turn, they are $k_w = 4.3$ rad/m and $\omega/2\pi = 2 \cdot 10^6$ Hz.

With allowance for the entire chain of furanose and benzene rings forming the RNA molecule, it is necessary to use Eq. (22) which describes the quasi-periodic redistribution of energy or complex FPU recurrence. In the experimental electronic model, we obtained an instantaneous pattern of such a recurrence in the form of a breather solution to the sine-Gordon equation with embedded high-frequency signal as can be seen in Fig. 3. Qualitatively, the computer solution (Fig. 2) and experimental picture (Fig. 3) are similar.

Thus, within the framework of the proposed electronic model, the RNA molecule can be treated as a carrier of the complex FPU recurrence. However, as distinct from the classical picture of the FPU recurrence [4], in the RNA model chain, the FPU spectral dynamics has a kind of fractal substructure due to the existence of microrecurrence in two interacting pairs of turns simulating interaction between the fields of furanose and benzene rings, whereas macrorecurrence occurs in the entire chain.

The next step in simulation consists in transferring the FPU spectrum of the RNA molecule to the nerve spike. For this purpose, we have to simulate the process of interaction between the ion-acoustic dynamics in the electrolyte of the neuron intracellular fluid and the electroacoustic FPU spectrum emerging in the neuron RNA molecule. By definition [16], a strong electrolyte represents an intermediate state between a crystal lattice of ions and random motion of ions in the solution. Strong electrolytes exhibit nonlinear dependence of conductivity on applied electric field [45]. To simulate this property, we chose a ferromagnetic material (a ferrite) to play the role of the strong electrolyte of the neuron intracellular fluid. Ferrite possesses ferroelectric, ferromagnetic, and semiconductor properties. The structure of ferrite consists of chaotically oriented inclusions (islands) of the FeO and Fe_2O_3 crystals in which some Fe atoms are replaced by atoms of Mn, Zn, Ni, and Co. The property of spontaneous polarization existing in ferrites provides the possibility for simulating the electric field dynamics in ferrite core as described by the NLS equation [46]. In the second stage of the experiment, therefore, we replaced the plastic toroidal core by the standard Mn–Zn ferrite core having the same size and $\mu = 3000$. To investigate the redistribution of energy in the lines, we analyzed the

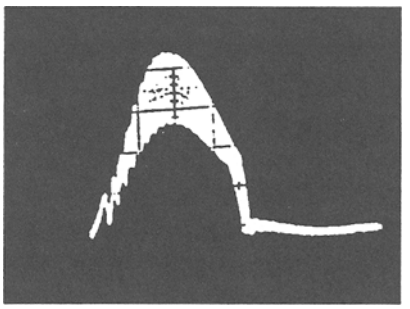

Fig. 4. The oscillogram of the voltage wave train illustrating the interaction between two pairs of lines wound on a ferrite toroidal core. Vertical axis: 10 V per division. Horizontal axis: 2 μs per division.

output waveforms with a DP2406 fast-Fourier real-time spectrum analyzer within the range of 0–70 000 Hz.

The FPU dynamics was experimentally observed in the resulting electromagnetic field of the two long transmission lines wound on the ferrite toroidal cores; one of the lines was tuned to the range of ferroacoustic resonance and the other, in the range of ferromagnetic resonance. Figure 4 shows the resulting oscillogram of interacting fields and Fig. 5 illustrates quasi-periodic Fourier image variations of the complex FPU recurrence. In the electronic model, the memory effect in this system is accounted for by the formation of an identifiable repeating pattern in the Fourier harmonic frequency distribution over a number of recurrences. Similar effects may be observed in strong electrolytes, dense plasmas, and in materials with mobile structure [47].

Mechanism of energy exchange between electromagnetic and acoustic waves in ferrite can be considered in the following way: Due to the island structure of the ferrite, the corresponding energy balance for the photons and phonons in the islands at the frequencies of ferroacoustic and ferromagnetic resonances can be defined as

$$2\mu H_n = \hbar\omega_{||}(k_{||})_{\text{photon}} = \hbar\omega_{|}(k_{|})_{\text{photon}}, \tag{32}$$

where $\omega_{|}$, $\omega_{||}$, $k_{|}$, and $k_{||}$ are the transverse and longitudinal temporal and spatial frequencies, respectively.

Equation (32) shows that the exchange of energy between electromagnetic field and acoustic field in the islands is realized via spin waves [48]. Furthermore, every island acts as a diffraction hole (of diameter d) for electromagnetic waves with the dispersion relation written as

$$\omega_1 = \frac{2\sqrt{2\pi}c}{d}\left|\frac{\sin(k_{|}d/d)}{k_{|}}\right|. \tag{33}$$

Equating the electromagnetic- and acoustic-field energies and using the expression $p = \hbar k$, we arrive at

$$\frac{2\sqrt{2\pi}c}{d}\left|\frac{\sin(p_{|}d/2\hbar)}{p_{|}/\hbar}\right| = 2\hbar\sqrt{\frac{X}{m}}\sin\left|\frac{p_{||}a}{2\hbar}\right|. \tag{34}$$

where a is the distance between neighboring atoms in the island, m is their mass, and X is the corresponding coupling constant.

For $d \gg a$, Eq. (34) for has many solutions and, with allowance for the uncertainty relation $\delta N \delta\gamma > 1$ for electromagnetic waves having phase γ and consisting of N quanta, we may infer that the energy spectra of interacting fields in an ensemble of islands in the ferrite toroidal core will exhibit low-frequency quasi-periodic broadening and narrowing, i.e., a complex FPU recurrence.

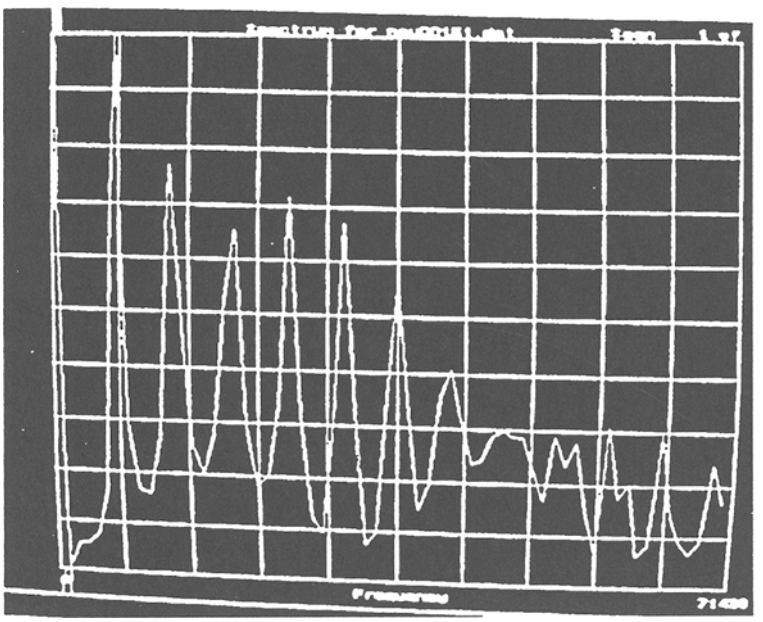

a

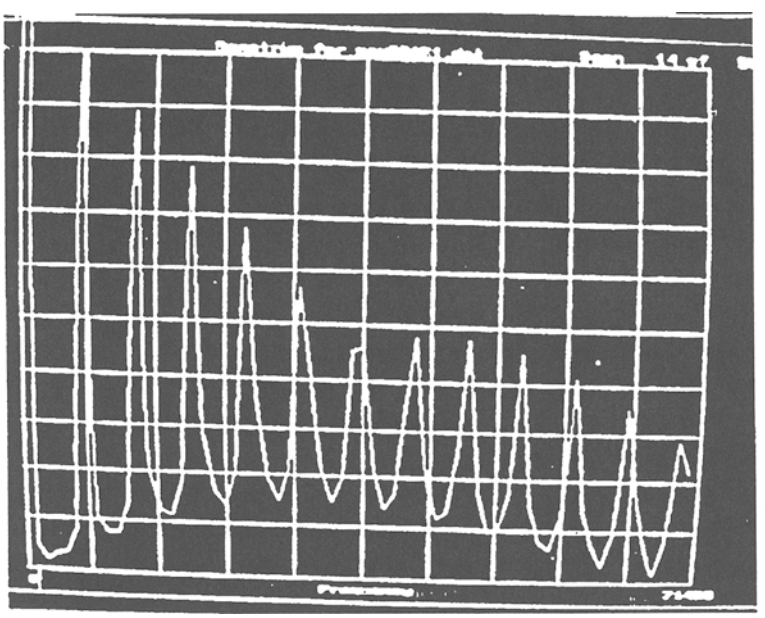

b

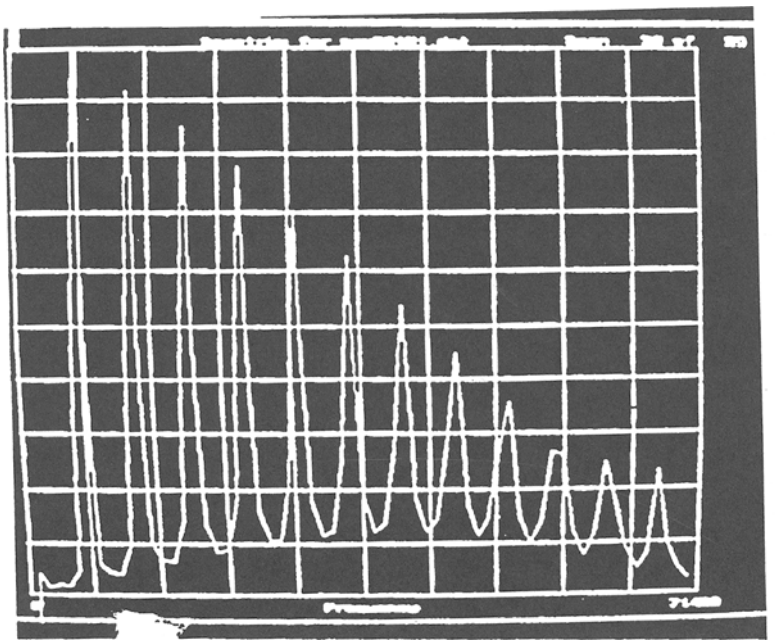

c

Fig. 5. Instantaneous Fourier images of the complex Fermi–Pasta–Ulam recurrence spectrum formed as a result of interaction between two transmission lines wound on a ferrite toroidal core. Vertical axis: power density spectrum (in arbitrary units). Horizontal axis: frequency (7.1 kHz per division). Exposure time is 100 μs, total number of scans is equal to 50, after one scan (a), after 14 scans (b), and after 29 scans (c).

In the model under consideration, the ferrite core plays the role of the intracellular strong electrolyte. As a result, according to (31), in both pairs of transmission lines tuned to the frequencies of ferroacoustic and ferromagnetic resonances, the micro FPU recurrence is incorporated into the macro FPU spectrum simulating the transfer of fractal substructure of the RNA FPU recurrence spectrum to the internal structure of the nervous spike. It is evident that every stimulation of a neuron results in incorporation of only a fraction of this spectrum into a spike. The most likely parts of the FPU spectrum to be incorporated in a spike are those related to memorization of the most habitual events and actions, such as mother tongue patterns, circumstances at home, and so on.

Thus, a neuron can be treated as a complex FPU electroacoustic resonator where the property of memory is simulated via a quasi-periodic redistribution of energy among the modes of electric and acoustic fields in the RNA molecule. Such a memory system does not have any limit in the body of information recorded. New information is merely incorporated into existing ones.

6. Discussion

Based on the model proposed, we may state that the existing Hodgkin–Huxley paradigm can be expanded by using (i) Hyden's idea about the role of the RNA molecule in neural information processing and (ii) a nonlinear approach which includes FPU recurrence as a key phenomenon for possible interpretation of the dynamic memory in a neuron. The process of modeling included the following steps:

(I) Deduction of equations which simulate the dynamics of Na, Cl, H, and OH ion concentration in the

intracellular neuron fluid;

(II) Simulation of the mechanism of short- and long-term memory as the FPU spectrum recurrence dynamics in the neural RNA molecule coupled with ionic fluxes in the intracellular fluid;

(III) Combination of all mechanisms into a single model, which makes it possible to describe the action potential as a soliton exhibiting an internal structure in the form of the FPU recurrence;

(IV) Numerical and experimental study of the model.

Description of the action-potential formation in a neuron as a sodium-concentration soliton which traps high-frequency oscillations of the proton concentration is similar to that of the plasma phenomenon of trapping Langmuir oscillations in the regions of low ion density as experimentally demonstrated by Ikezi [27]. Coupling the sine-Gordon to the KdV equations for the simulation of this mechanism is also within the framework of the mentioned approach [27].

We next considered a neuron RNA molecule as a main carrier of information and simulated by a chain of nonlinearly coupled oscillators: furanose ring generating acoustic waves and benzene ring producing electric waves. Replacement of nitrogen base by benzene ring represents an evident simplification of the problem. However, for the phenomenon of the FPU recurrence, it does not make much difference because the allowance for concrete nucleotide sequences in the RNA molecule model brings about only individual characteristics for a certain molecule without changing the concept of the FPU recurrence as an information carrier.

Quantum-mechanical description of the dynamics in the coupled furanose and benzene rings was necessary to demonstrate two levels of data storage in the RNA molecule: the micro and macro ones. Coupling the sine-Gordon with the NLS equations for simulation of this mechanism is based on the classical quantum-mechanical approach and nonlinear generalization of the Zakharov couple.

Numerical and analog experiments were aimed at the verification of the proposed model and proved the existence of realistic solutions of the mentioned couple of equations in both numerical and analog forms. During the analog experiment a new property of the FPU recurrence has been observed: the presence of fractal substructure in the FPU spectrum, which may extend to the quantum scales of spatial and temporal frequencies of the recurrence spectrum. But this requires further consideration.

Summing up, we can state that the model proposed may be useful for developing artificial neurons. As a concluding remark, we express our believe that, if such a mechanism does exist, it is of artificial origin.

Acknowledgments

We thank the Princeton University for its understanding and guidance in the solution of the problem from the very early stage and the John Fetzer Foundation for its financial support.

References

1. A. L. Hodgkin and A. F. Huxley, *J. Physiol.* (London), **117**, 500 (1952).
2. H. Hyden and E. Egyhazi, *Proc. Natl. Acad. Sci. USA*, **52**, 1030 (1964).
3. H. Hyden and P. W. Lange, *Exp. Cell. Res.*, **62**, 125 (1970).
4. E. Fermi, J. Pasta, and S. Ulam, in: *Collected Papers of Enrico Fermi*, Chicago University Press (1955), Vol. 2, p. 978.
5. H. C. Yuen and W. E. Ferguson, *Phys. Fluids*, **22**, 2116 (1978).
6. J. Ford and J. Waters, *J. Math. Phys.*, **4**, 1293 (1963).
7. J. Tuck and M. Menzel, *Adv. Math.*, **9**, 399 (1972).
8. R. M. Livi, S. Pettini, M. Ruffoo, et al., *Phys. Rev.* A, **31**, 1039 (1985).
9. D. S. Sholl and B. I. Henry, *Phys. Rev.*, A**44**, 6364 (1991).

10. N. J. Zubusky and M. D. Kruskal, *Phys. Rev. Lett.*, **15**, 240 (1965).
11. H. C. Yuen and B. M. Lake, in: *Solitons in Action*, Academic Press, New York (1978), p. 89.
12. M. Pettini and M. Landolphi, *Phys. Rev.* A, **41**, 768 (1990).
13. A. Berezine, *J. Phys.* D, **22**, 577 (1989).
14. J. M. Luck and A. Mehta, *Phys. Rev.* E, **48**, 3988 (1991).
15. H. S. Frank and W. Y. Wen, *Disc. Faraday Soc.*, **24**, 133 (1957).
16. V. V. Skorcheletti, *Theoretical Electrochemistry*, Goskhimizdat, Leningrad (1963).
17. M. Toda, *J. Phys. Soc. Jpn*, **22**, 431 (1967); **23**, 501 (1967); **35**, 101 (1969); **34**, 18 (1973); *Phys. Rep.*, **10**, 1 (1975).
18. A. C. Damask, *Medical Physics*, Academic Press, New York (1978), Vol. 1.
19. I. S. Gonorovsky, *Electronic Circuits and Signals* [in Russian], Sovetskoe Radio (1967), Vol. 1.
20. F. S. Barnes and Chia-lun J. Hu, in: *Nonlinear Electromagnetics*, Academic Press, New York (1980).
21. U. B. Americ and B. A. Kretsel, *Chemistry of Liquid Crystals and Mesomorphous Polymer Systems*, Nauka, Moscow (1981).
22. Ja. I. Frenkel and T. A. Kontorova, *Zh. Teor. Éksp. Fiz.*, **8**, 89 (1938).
23. A. S. Davydov, *Solitons in Molecular Systems* [in Russian], Naukova Dumka, Kiev (1988).
24. E. N. Pelinovskii, *Radiofizika*, **XIX**, 883 (1976).
25. T. A. Fulton, in: *Superconductor Applications: SQUIDs and Machines*, Plenum Press, New York (1977).
26. A. C. Scott, "Birth of Paradigm," in: *Solitons in Action*, Academic Press, New York (1979).
27. H. Ikezi, "Solitons in plasmas," in: *Solitons in Action*, Academic Press, New York (1979).
28. H. Hyden and P. W. Lange, *Exp. Cell. Res.*, **62**, 125 (1970).
29. H. Hyden and P. W. Lange, *Proc. Natl. Acad. Sci. USA*, **65**, 898 (1970).
30. H. Hyden and P. W. Lange, *Proc. Natl. Acad. Sci. USA*, **69**, 1980 (1972).
31. C. Altona and M. Sungaralingam, *J. Am. Chem. Soc.*, **94**, 8205 (1972).
32. J. F. Currie, S. E. Trullinger, A. R. Bishop, and J. A. Krumhansl, *Phys. Rev.* B, **15**, 5567 (1977).
33. A. J. Lichtenberg and M. A. Lieberman, *Appl. Math. Sci.*, Springer (1991), Vol. 38, p. 450.
34. R. P. Feynman, R. B. Leighton, and M. Sands, *The Feynman Lectures on Physics*, Addison-Wesley, London (1963), Vol. 3.
35. E. J. Heller, *J. Chem. Phys.*, **62**, 1544 (1975).
36. M. J. Davis and E. J. Heller, *J. Chem. Phys.*, **75**, 3916 (1981).
37. M. Henon and C. Heiles, *Astron. J.*, **69**, 73 (1964).
38. M. J. Davis, E. B. Stechel, and E. J. Heller, *Chem. Phys. Lett.*, **76**, 21 (1980).
39. V. I. Petviashvili and O. A. Pochotelov, *Solitary Waves in Plasmas and the Atmosphere* [in Russian], Atomizdat, Moscow (1989).
40. G. P. Berman and A. R. Kolovskii, *Sov. Phys. JETP*, **60**, 1116 (1984).
41. V. E. Zakharov, *Sov. Phys. JETP*, **62**, 1745 (1972).
42. L. L. Goldin and G. I. Novikova, *Introduction to Quantum Physics* [in Russian], Nauka, Moscow (1988).
43. R. D. Parmentier, "Fluxons in distributed Josephson contacts," in: *Solitons in Action*, Academic Press, New York (1979).
44. V. I. Kalinin and G. M. Gerstain, *Introduction to Radiophysics* [in Russian], GITTL, Moscow (1957).
45. M. Wien, *Phys. Zs.*, **32**, 545 (931).
46. G. L. Lamb and D. W. McLaughlin, *Solitons*, Springer, Berlin (1980).
47. J. Dumas, *Phys. Rev.* B, **30**, 2249 (1984).
48. M. Warden, *Phys. Rev.* E, **48**, R639 (1993).